Exploring the Conformational Space of Vpu from HIV-1: A Versatile Adaptable Protein

JENS KRÜGER, WOLFGANG B. FISCHER
Institute of Biophotonics, School of Medical Science and Engineering, National Yang Ming University, 155, Sec. 2, Li-Nong St., Taipei 112, Taiwan

Received 7 January 2008; Accepted 26 February 2008
DOI 10.1002/jcc.20986
Published online 23 April 2008 in Wiley InterScience (www.interscience.wiley.com).

Abstract: The dynamic behavior of monomeric Vpu_{1-32} from HIV-1 in different lipid environments has been studied. The peptide shows highly flexible behavior during the simulations and easily adapts to changing lipid environments as it experiences when travelling through the Golgi apparatus. Protein–lipid interactions do not show any significant correlation towards lipid type or thickness based on multiple 10 ns simulations. The averaged structure of a series of 16 independent simulations suggest kink around Ser-24, which compensates the polarity of its side chain by forming hydrogen bonds with the carbonyl backbone of adjacent amino acids towards the N-terminus.

 J Comput Chem 29: 2416–2424, 2008

Key words: Vpu; HIV-1; membrane proteins; protein stability; lipid bilayers; MD simulations

Introduction

Viruses invade their host and tune the cellular production machinery to its own benefit. In this respect, viruses follow two strategies: (i) they induce changes in chemical or electrochemical gradients by changing the permeability of the lipid membrane in respect to ions and small molecules or (ii) they modulate host cell response by interacting with e.g., membrane proteins from the host.[1,2] These "modulating" proteins are encoded by the viruses amongst them those who form channels or pores. These latter protons are usually small with around 100 amino acids in length, with the so far only known exception of 3a from SARS-CoV of almost 300 amino acids.[3]

For some viruses, these proteins are essential such as M2 for influenza A[4–6] or p7 for hepatitis C virus[7] for some of them the virus can replicate without them, such as without its HIV-1 Vpu,[8] but to a significant lower extend. There is an emerging common sense about all the channel proteins, in that they have to assemble to function as a channel or pore.

The proteins are expressed in the rough endoplasmic reticulum (ER). From there they are translocated to their place of action. And it is exactly at this place in the ER where questions arise: (i) after being expressed, do these proteins exist as monomers for a considerable time in the ER or even remain as single monomers until they reach their target site; (ii) independent of that, how many of them do assemble and if so, how is this achieved? It is especially the latter question which demands an answer about the conformation these proteins adopt in their monomeric state prior to assembly.

In this respect, the pore forming protein Vpu from HIV-1 is chosen to elucidate the root of action at the molecular scale. Vpu is a 81 amino acid type I integral membrane protein[8,9] found in subcellular units of infected cells.[10,11] Two functions are known[12,13] to be associated with two topologically distinct regions of Vpu.[14] The transmembrane (TM) domain is essential to facilitate the release of the newly emerging virus particles.[15,16] This seems due to the homo-oligomerization of the protein[17] consequently inducing channel activity[15,16] and/or by interaction with other host cell ion channels. The second role of Vpu is to initiate the down regulation of the CD4 receptor for which the cytoplasmic part is responsible.

The structural picture of Vpu is based on solution[18,19] and solid state NMR,[20–22] CD,[23] and FTIR spectroscopic investigations.[24] In these investigations, a helical transmembrane domain is proposed, while the cytoplasmic domain comprises of two helices. In dependence of the experimental conditions under which the solution NMR data was taken, residues from Pro-75 onward adopt either a turn[18] or a helix[19] motif. These structural information have been used for computational measurements such as molecular dynamics (MD) simulations to derive insight into the mechanism of function of these proteins on an atomistic level.[25–30]

Correspondence to: W. B. Fischer; e-mail: wfischer@ym.edu.tw

Contract/grant sponsors: National Yang-Ming University; Taiwanese government (Aim-of-Top University Plan); National Science Council (NSC) of Taiwan

There has been experimental evidence that Vpu_{1-32} and consequently the full length protein as well, when assembled to form pores, may straighten to open.[31] No starting condition of such a gating process is known. Nevertheless, this type of gating would ask for mechanical flexibility of the protein. To dissect the complex mechanism in the present study molecular dynamics (MD) simulations are used to address the flexibility of the monomeric unit[28,32] within different membrane environments. This study allows assessing the hypothesis that Vpu—and the viral channel forming proteins in general—diffuses as a monomeric unit prior to the assembly either with itself or with other target proteins such as CD4 or the TASK channel.

Computational Method

Ideal helices ($\phi = -65^\circ$ and $\psi = -39^\circ$) of Vpu_{1-32} (MQPIPI-VAIV[10] ALVVAIIIAI[20] VVWSIVIIEY[30] RK) have been generated using MOE (www.chemcomp.com) and its integrated protein builder. A prekinked peptide has been generated by changing the values for the backbone dihedrals of Ser-24 to $\phi = -50^\circ$ and $\psi = -25^\circ$. This procedure resulted in a 7° kink of the otherwise ideal helix, which is in accordance with experimental findings.[33]

The peptides were embedded into lipid bilayers by cutting out six overlapping lipid molecules using the modeling program MOE. The lipid - protein system has then undergone multiple energy minimization steps (Gromacs) followed by short MD simulations (up to 400 ps) with positions constraints on the peptide.

The peptide was simulated in four different lipid environments (DPPC, POPC, DTPC, and DDPC). The helical monomers were either placed in the membrane aligned parallel to the membrane normal (0°), or pretilted with a tilt angle of 25° (see also[34]). The kink around Ser-24 was chosen to be either 0 or 7°. Thus, four different simulations were run for each lipid composition (in total 16 independent simulations were carried out).

Topologies for four lipid bilayers (DPPC (16:0 Diester PC, 1,2-Dipalmitoyl-*sn*-Glycero-3-Phosphocholine, POPC (16:0-18:1 Diester PC, 1-Palmitoyl-2-Oleoyl-*sn*-Glycero-3-Phosphocholine, DTPC (14:0 Diether PC, 1,2-Di-O-Tetradecyl-*sn*-Glycero-3-Phosphocholine, DDPC (10:0 Diester PC, 1,2-Didecanoyl-*sn*-Glycero-3-Phosphocholine) were created on the basis of the parameters by Chandrasekhar et al.[35] Using the modeling software MOE and its scripting vector language (SVL), the lipid molecules were placed in such a way that they form a bilayer, while their rotational orientation was randomized. The systems consisting 128 lipid and 3655 water molecules, were stepwise minimized and equilibrated (5–10 ns).

GROMACS-3.3.1 with the Gromos96 (ffG45a3) forcefield was used for the simulations with an integration stepsize of 2 fs. The temperature of the peptide, lipid, and the water molecules were separately coupled to a Berendsen thermostat with a coupling time of 0.1 ps. Fully isotropic pressure coupling was applied with a coupling time of 1.0 ps and a compressibility 4.5×10^{-5}. Long range electrostatics were calculated using the particle-mesh Ewald (PME) algorithm with grid dimensions of 0.12 nm and interpolation order 4. Lennard-Jones and short-range Coulomb interactions were cut off at 1.4 and 0.8 nm, respectively. The final (pre-)equilibrated simulation system consisted of Vpu_{1-32}, 122 lipid molecules for all membranes used in this study and 3650 water molecules in a periodic rectangular box. In addition to the six lipid molecules, which overlapped with the peptide also five water molecules had to be removed. The total number of atoms per simulations was in the range of 15890–17354 depending on the lipid type.

Except for the root mean square displacement (RMSD) plots, all other plots were generated over the last 4 ns of each 10 ns simulation. The tilts and kink are measured over the center of mass of the backbone of residues 5–8, 20–24, and 25–28. Numerical data, such as lipid thickness and area per lipid, have been extracted using GROMACS tools.

Principal component analysis (PCA) was carried out using the program g_covar from the GROMACS-3.3.1 package. The covariance matrix of positional fluctuation was computed for the last 4 ns of each simulation for the mainchain and C_β-atoms of residue 5–28. The overall rotational and translational motions were removed by fitting the peptide structure of each time frame to the starting structure. The overlap of the different covariance matrices was computed pair wise between all simulations with g_anaeig also from the GROMACS-3.3.1 package.

In total simulations, over more than 430 ns (or 165,000 cpu h) were prepared on a DELL Precision 490n workstation and run on facilities of the Paderborn Center for Parallel Computing PC^2 (http://wwwcs.uni-paderborn.de/pc2/).

Plots and pictures were generated using xmgrace, MOE, VMD, POV-Ray, and blender.

Table 1. Average Values from 70 ns Equilibrium Simulations of 2×64 Lipid Bilayers with Isotropic Pressure Coupling at 310 K in Comparison with Experimental Data.

		DPPC (16:0)	POPC (16:0–18:1)	DTPC (ether 14:0)	DDPC (10:0)
Lipid thickness (Å)	Simulation	35.5 ± 0.6	36.1 ± 0.6	34.4 ± 0.5	27.8 ± 0.7
	Experiment	37 (at 44°C)[38]	38 (at 20°C)[38]	–	26.5 (at 20°C)[38]
Area per lipid (Å^2)	Simulation	62.66 ± 0.01	63.62 ± 0.01	57.65 ± 0.03	55.00 ± 0.08
	Experiment	63.3 (at 50°C)[37]	–	–	–

The agreement between experiment and simulation lies within in the error range of both. The lipid thickness refers to the differences between the centers of mass of the phosphorous atoms in each leaflet. The standard deviation derives from averaging over all time frames.

Table 2. Data from 10 ns Equilibrium Simulations of 2 × 64 Lipid Bilayers and Vpu_{1-32}.

		DPPC (16:0)	POPC (16:0–18:1)	DTPC (ether 14:0)	DDPC (10:0)
Ideal helix	0° starting tilt	34.5 ± 1.1	33.8 ± 1.1	32.4 ± 1.1	27.0 ± 0.9
	25° starting tilt	34.4 ± 1.1	33.9 ± 1.1	32.5 ± 1.0	28.4 ± 0.9
Prekinked	0° starting tilt	33.7 ± 1.1	33.9 ± 1.1	32.5 ± 1.0	27.2 ± 0.9
	25° starting tilt	33.7 ± 1.1	33.9 ± 1.1	32.5 ± 1.0	27.0 ± 0.9

Within the error of the simulation, no significant difference towards the simulation without peptide is observable.

Results

The following data illustrates the dynamic behavior of Vpu_{1-32} from HIV-1 in different lipid environments. The adaptation to the hydrophobic core of the lipid membrane requires flexibility and the compensation of unfavorable contacts.

Lipid

All lipid data (Table 1) were derived from 70 ns simulation of the fully equilibrated system. The patches remain stable throughout the simulation time and adopt thicknesses between 28 and 36 Å. The simulation data fit extremely well within the experimental data, were available.[36–38]

In detail, the thickness of the POPC and DPPC bilayer adopt values of 36.1 Å ± 0.6 and 35.5 Å ± 0.6, respectively, whilst DDPC with the shortest lipid chain length of 27.8 Å ± 0.7. The area per lipid is for DDPC the smallest with 55.00 $Å^2$ ± 0.08 and the largest for POPC and DPPC with 63.62 $Å^2$ ± 0.01 and 62.66 $Å^2$ ± 0.01, respectively. DTPC, as the only ether among the simulated lipids, adopts a thickness of 34.4 Å ± 0.5 and an area per lipid of 57.65 $Å^2$ ± 0.03.

After insertion of the peptide and consecutive 10 ns of simulation, the lipid thickness is only marginally decreased for all patches (Table 2). There is no direct influence of the peptides conformation or orientation on the lipid thickness. For the simulations with a 25° starting tilt angle, the pattern with the DPPC bilayer being the thickest patch with values of 34.4 Å ± 1.1 and 33.7 Å ± 1.1 and DDPC being the thinnest patch with values of 28.4 Å ± 0.9 and 27.0 Å ± 0.9 remains. A sequence of decreasing thickness follows DPPC ≥ POPC > DTPC > DDPC independent of the presence and the conformation of an inserted peptide. Membrane deformation due to the inserted peptides can be denied under the current computational conditions.

Peptide

In all 16 independent simulations, Vpu remains stable in the lipid bilayers in an overall helical conformation independent of the starting tilt angle (0 or 25°) and the kink angle (0 and 7°). The RMSD plots for the C_α atoms show a rise within the first nanosecond followed by various fluctuations between 0.3 and 0.4 nm for the untilted (0°) simulation (for representative values see Fig. 1). Tilting of the helix and partial unwinding of up to four residues at either ends facing the lipid/water interface is responsible for this effect,[32,39] but the overall helical motif remains intact. For the pretilted simulation (25°) the values level off at around 0.16 nm indicating a stable system (see Fig. 1). The peptide conformation is such that the polar and/or charged residues Met-1, Gln-2 at the N-terminus and Glu-29, Tyr-30, Arg-31, Lys-32 at the C-terminus anchor the protein within the lipid head group region (see Fig. 2). The root mean square fluctuation (RMSF) of these terminal residues is higher than for the core amino acids (data not shown), which supports experimental findings of the flexibility in these regions.[40] On the basis of the findings in these simulations that the peptide kinks around Ser-24 the simulations with a "pretilted" helix of 25° have also been done with the helix "prekinked" around Ser-24.

Protein TILT

It takes about 6 ns until the peptide can reach an equilibrium tilt, starting from 0°. Starting from the simulation with an already tilted conformation of 25° relative to the membrane normal, this equilibrium tilt can be reached in less than 2 ns. Whether the peptide is prekinked around Ser-24 or not, has no impact on the equilibration time. Nevertheless all further analysis is based on the last 4 ns of each 10 ns simulation, to assure as much as possible being in an equilibrium state. In the following

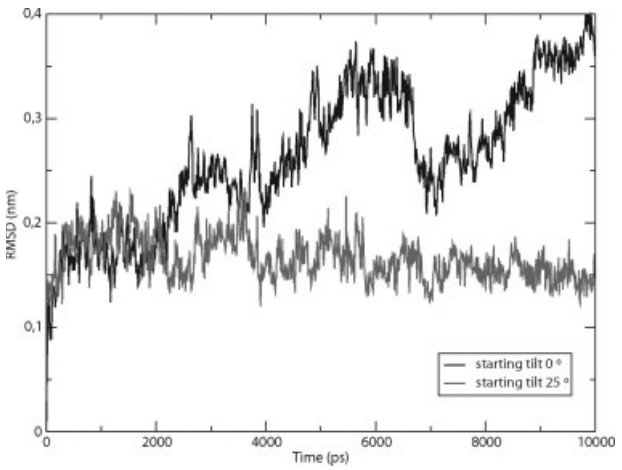

Figure 1. Representative RMSD plot for helices inserted with no tilt (0°, black line) and an initial tilt of 25° (grey line). This plot refers to simulations in DDPC, but also for the other lipid compositions similar behavior is observed.

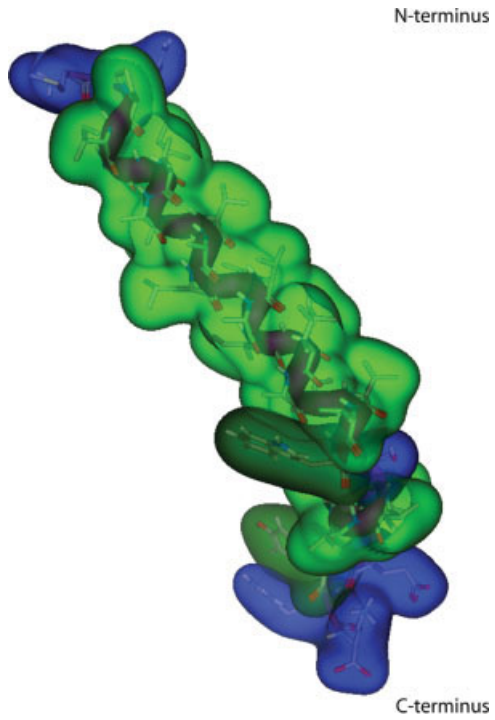

Figure 2. Sidechain polarity relevant for the arrangement of Vpu_{1-32} between polar lipid headgroups and hydrophobic carbon tails of a representative conformation (hydrophobic light green, hydrophilic or charged blue, aromatic dark green).

analysis, only those data from simulations with the pretilted helices are therefore considered further to avoid the interpretation of the data based on undesired conformational effects such as unwinding at the termini, which are exposed to the solvent.

The tilt and kink are measured as illustrated in Figure 3A using the center of mass of the backbone of residues Pro-5 to Ala-8, Ile-20 to Ser-24, and Ile-25 to Ile-28. A representative equilibrium conformation is shown in Figure 3B. Beside the C- and N-terminal ends all residues are covered with lipid, promoting an overall helical structure. The calculated tilt angles vary with the membrane type and lie within a range of 20–50°, which agrees with experimental findings.[34] For POPC and DDPC, the tilt angle remains almost the same towards the end of the simulations with values of about 25° or, respectively, 28°, although the lipid is 6 Å thinner in the latter case (Figs. 4B and 4D). Simulations in DPPC and DTPC show a stable but fluctuating tilt angle with values about 42 and 38°. The amplitude of the fluctuation can be as high as 10° (Fig. 4A) but also less than 5° (Fig. 4C). For these values, no correlation with the lipid thickness has been observed. It is also irrelevant whether the peptide was prekinked or not.

Protein KINK

The kink measured as illustrated in Figure 3A indicates the bend of the helical axis over Ser-24. During the simulations this is the most prominent structural feature, but there is also some bending being observed involving residues Ile-20 to Ser-24. As the kink is pretty much at the C-terminal end of the peptide, it can undergo changes in the range of 5–60° without affecting the tilt or the overall stability of peptide (see Fig. 5).

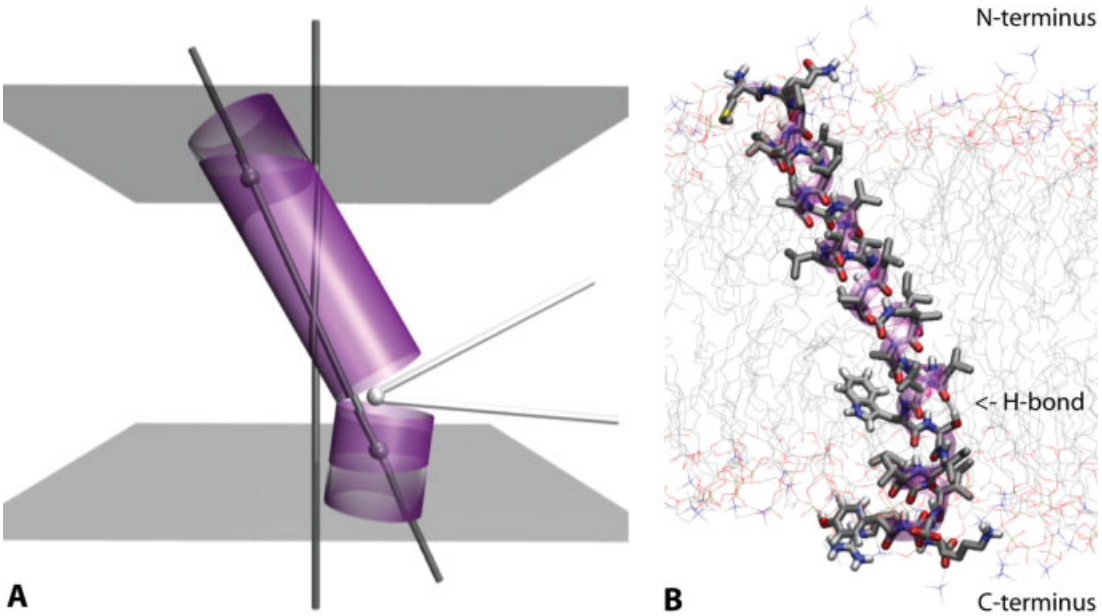

Figure 3. (A) Schematic sketch of equilibrated helical TM domain of Vpu. The tilt is indicated by the gray lines relative to the membrane normal, for the kink in white. The spheres show the position of the center of mass used for the analysis. (B) Vpu_{1-32} after 10 ns simulation time in DPPC. This representative frame shows the H-bond between Ser-24 and Ile-20. To clarify the representation water molecules are not shown.

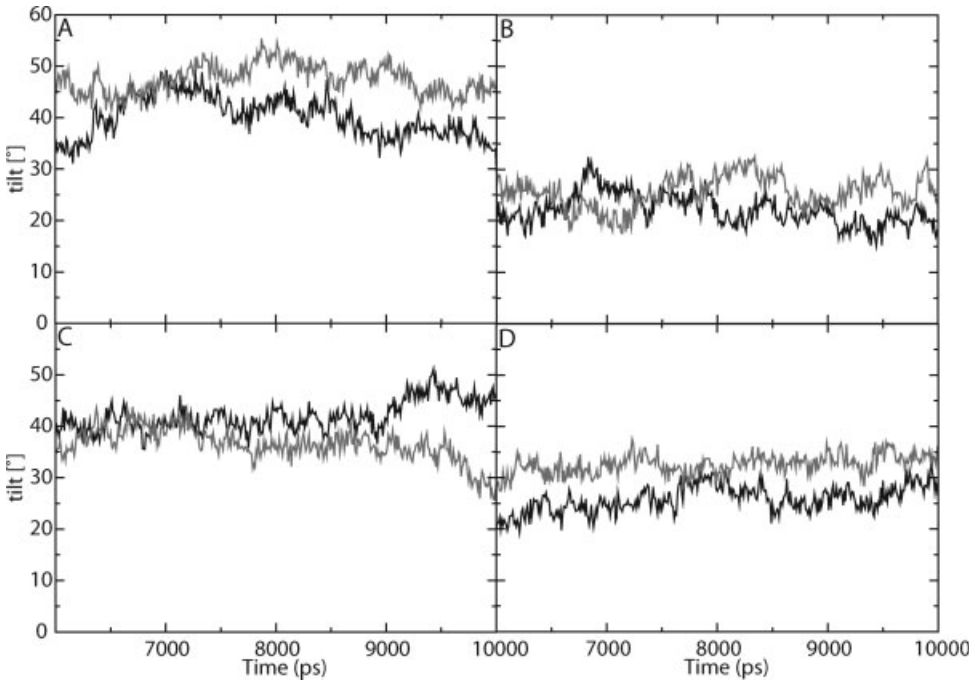

Figure 4. Tilt relative to the membrane normal for the different simulations over the last 4 ns of each simulation. (A) DPPC (B) POPC (C) DTPC (D) DDPC. The straight black line corresponds to the ideal helical starting conformation, the grey line to the prekinked. Simulations were started with a tilt of 25°.

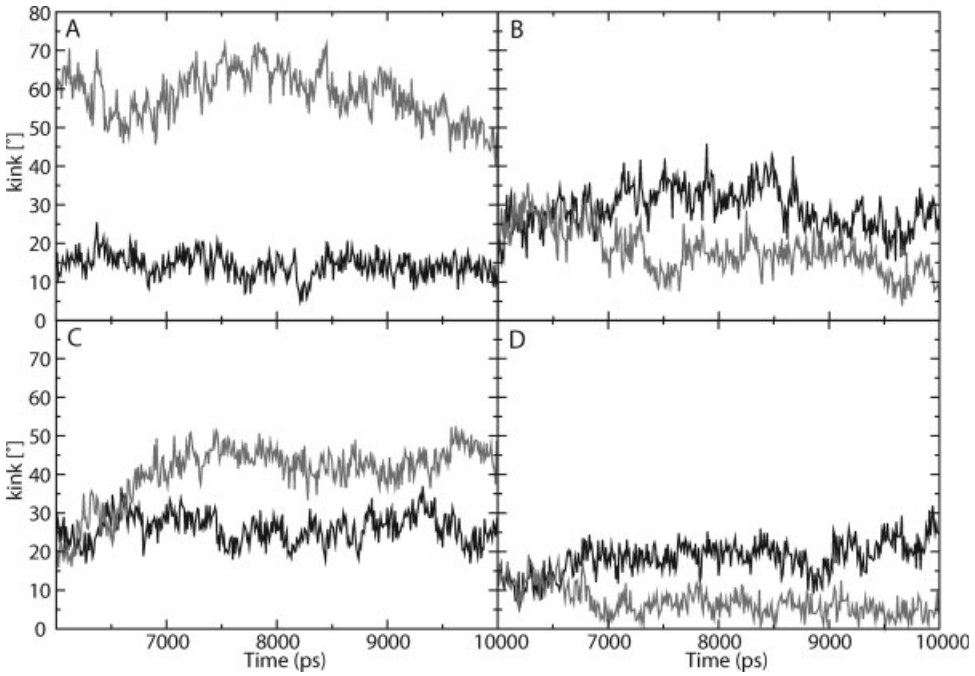

Figure 5. Kink over the residues 20–24 for the different simulations over the last 4 ns of each simulation. (A) DPPC (B) POPC (C) DTPC (D) DDPC. The straight black line corresponds to the ideal helical starting conformation, the grey line to the prekinked. Simulations were started with a tilt of 25°.

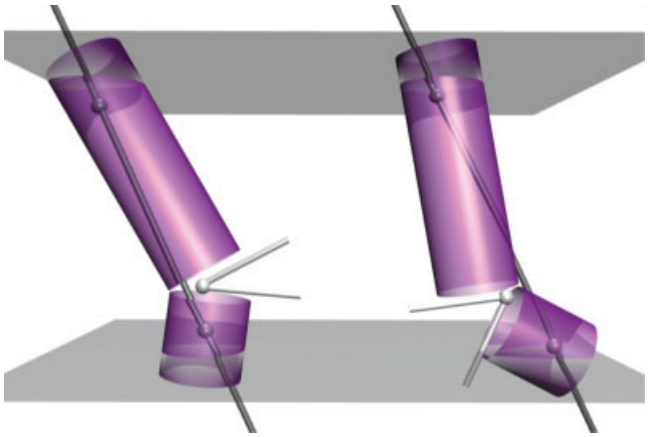

Figure 6. Illustration of how a rotational transition of the peptide around its helical axis enables different kinks (angle between the white lines), while the tilt (gray line, see also Fig. 3A) remains practically unchanged, as it is observed e.g., in the case of the simulations in DPPC.

The kink is stabilized by the formation of an internal H-Bond between the hydroxyl group of Ser-24 and the backbone carbonyl oxygen of either Ile-20 or Val-21 (Fig. 3B). During the simulation a reversible flipping of the H-bond from one carbonyl oxygen to the other could be observed, without affecting the kink angle. This compensation allows the helix to remain positioned within the hydrophobic core of the lipid membrane and with its hydrophilic part towards the C terminus in the lipid headgroup region.

Like the tilt, the kink also does not show any simple correlation with the lipid composition or thickness. Analyzing the tilt and kink angles show that both values easily change to allow a good hydrophobic cover of the peptide by the lipid bilayer. This leads to a situation as illustrated in Figure 6, where a rotational transition leads to two stable conformers having the same tilt but completely different kinks.

Conformational Space

PCA of the positional fluctuation during each simulation was carried out. The eigenvectors of the covariance matrices give the direction and eigenvalues quantify the magnitude of the fluctuation. The trajectory can be projected onto the eigenvectors; usually the first few represent most of the functional motions of the system. Pair wise comparison of all covariance matrices indicates that regardless of the specific lipid environment or starting conformation all simulations share the same conformational space, although the total overlap between the covariance matrices lies only within the range of 0.45–0.80. The analysis of the projection of the simulation trajectories on their eigenvector planes (data not shown) leads to an identical observation. Each single simulation does not cover the whole range of possible conformations, but all overlap with the common average structure, which is shown in Figure 7.

The main reason for this is the locally very ambivalent situation where the peptide is adapting to its lipid environment, which could be best described as "rolling" kink. While in some simulations a kink is barley observed, in other cases the kink angle is close to 70° (Fig. 5A). This is influencing the relative orientation of the peptide towards the membrane as it is illustrated in Figure 6. Depending on the different rotational orientation certain movements are preferred over others, e.g., movements along (parallel) the lipid tails, instead of against (perpendicular) them. Generalizing over all simulations the bending movement is the

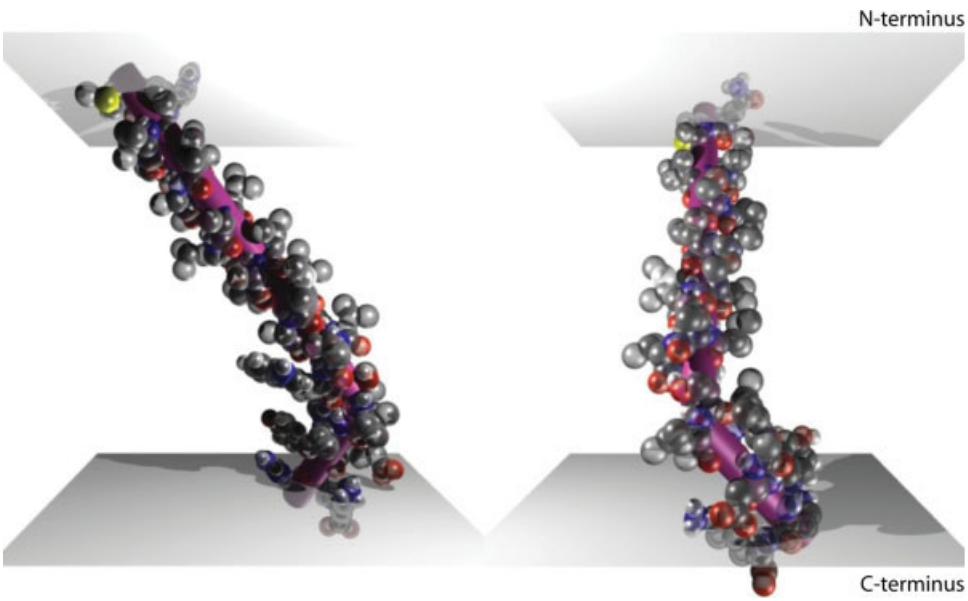

Figure 7. Average structure of Vpu. The purple rods indicate the principal helical axis. On the left, the upper longer rod lies in the image plane, while the shorter rod is pointing away from the viewer. On the right the view point was rotated by 90°, allowing a view from the side.

most prominent motion. The second largest movement is the orthogonal movement where the smaller kinked part is bending out of plane (see Fig. 7).

To summarize the findings, at least three angles are required to describe the orientation of Vpu correctly:

i. The tilt angle relative to the membrane normal measured over the whole peptide. A value of 37° can be considered as good average for phosphocholine lipid environments, which are used in NMR measurements.[34] Even in the same lipid this value can easily be lower or higher by 15°, which also applies for other lipids.
ii. The kink angle at Ser-24, between the two parts of the peptide, which usually lays around 32°.
iii. If the N-terminal (upper) part is considered to lie in the image plane (Fig. 7 left side), how far the C-terminal (lower) part is bend out of this plane (Fig. 7 right side). Values around 30° are observed.

Discussion

In this study, the peptide data analysis focuses on simulations with Vpu_{1-32} being pretilted by 25° relative to the membrane normal. This angle is a compromise for the data reported on Vpu peptides oriented in bilayers immobilized on glass plates with angles of 13°[33] and 27–51° with decreasing lipid thickness[34] as well as data reported from experiments with Vpu peptide in magnetically aligned bicelles with an angle of 30°.[41] Recent data on a Vpu_{1-40} peptide suggest a 13° tilt with the peptide in an oligomeric state[40] whilst MD Simulations with monomeric Vpu_{1-52} report on an angle of the TM domain of about 23°.[28] M2 peptide corresponding to the TM domain of the protein (influenza A) has been suggested to adopt angles in the range of 30–38°.[42–44]

The protein undergoes large movements during the simulations. There is no prominent single stable conformation. The first and last three to four residues show the highest flexibility, whilst the residues in between are less flexible, due to damping by the lipid.[40] The anchoring of polar residues in lipid headgroup forces the peptide into the lipid bilayer and does not allow an exposure of transmembrane residues to the aqueous phase.

The peptide as a monomer has thereby to adapt to the lipid thickness and tilts. Tilt angles between 10 and 50° relative to the membrane normal can be observed, while values around 37° are the most common and stable. There is no simple correlation between lipid thickness and tilt. The tilt and kink in each of the 16 independent simulations can undergo significant fluctuation. There is also no obvious correlation to the lipid types. The conformation of the hydrophobic central part is helical.[20,21,45] But as an ideal helix would be significant longer than the lipid thickness, the peptide has to tilt and/or to kink to achieve optimal interaction with the lipid environments. This picture remains intact even when varying the lipid length between 10 and 18 methylene units and changing the lipid type from diesters to diethers. The combination of small changes in tilt and kink angles in conjunction with rotation along its main axis is sufficient to allow the hydrophobic core part of Vpu be fully covered within the lipid tails.

The lack of a clear correlation between tilt and lipid thickness is just due the fact that the MD simulation and the NMR experiment were carried out on completely different time scales, nanoseconds in the first and milliseconds in the latter case. Furthermore in MD, an isolated monomer is studied, while in NMR relative high peptide concentrations are required. This may leads to (partial) peptide aggregation, which biases the structural data generated by this technique. Recent X-ray reflection and scattering experiments indicate that Vpu_{1-32} aggregates at a protein to lipid ratio of 0.02.[46] In fact, averaging over time and concentration shows that both, simulation and experiment deliver complemental results.

A hydrophobic mismatch in the classical sense, with the peptides affecting lipid thickness in its immediate environment,[47–49] can not be observed although suggested by others using X-ray reflectivity measurements.[46] The compensation seems to be taken care by the peptide alone. Monomeric Vpu simply avoids unfavorable contacts by tilting, in combination with a variable kink around Ser-24. A significant deformation of the membrane can not be observed throughout the simulations.

The majority of simulations show the formation of a significant kink in the range of residues Ile-20 to Ser-24. The hydroxyl group of Ser-24 forms a dynamic hydrogen bond with the backbone carbonyl oxygen of Ile-20 or Val-21. This appears to induce and stabilize the observed kink in this region. This kink is almost two turns away from the proposed bend around Ile-18 reported by NMR spectroscopy (Ile-17 in[33]). This discrepancy may result from the use of different lipid composition (use of dioleoyl lipids (DOPC and DOPG[33]) but also the use of the poly-Gly-Lys linker at the C terminal end. This latter suggestion seems to find support in MD simulations with monomeric Vpu_{1-52}[28] in which a bend closer to the experimentally found residue, Ile-18,[33] has also been observed. It may thus been concluded that the extension of the TM domain with the extramembrane part of the protein affects the structure of the TM domain and consequently also the channel kinetics (elongated open time) when forming a bundle.[31,50] This is a further indication of conformational flexibility of the TM domain of Vpu.

Vpu_{1-32} shows two kinds of prominent dynamic movements. Both involve bending over the kink, while one is in plane and the other out of plane. Depending on the relative orientation towards the lipid tails, one of the two is always more damped than the other. These movements show again how easy and flexible Vpu_{1-32} can adapt to changing lipid environments. It also suggests that bundle formation leads to a "stiffening" of the helices as suggested from NMR experiments with Vpu_{1-40} peptides.[40] This conformational change could be possible if the energy barrier to alter the conformation of the TM domain is low.

In a similar way, Alamethicin also adopts to its lipid environment. Kink and tilt angles of similar range have been reported in MD simulations when it is inserted into either a lipid bilayer or an octane slab.[51] *In silico* studies of embedding, the TM domain of the lactose permease, LacY, into a lipid bilayer, also reports on a peptide-driven adjustment to hydrophobic mismatch with the bilayer.[52] In contrast, computational simulations on synthetic monomeric model peptides (repeating units of KALP (single letter code)) embedded in lipid bilayer patches of various lengths[53] report that the peptide remains kink-free and in an

α-helical conformation. The peptide rather tilts to compensate for the mismatch. NMR spectroscopic investigations suggest that this large tilt may be due to the lysines when compared with similar peptides where the lysine is replaced by tryptophans.[54]

It seems likely that some peptides undergo kinking in addition to a pure tilt for the compensation of the mismatch, which obviously is driven by energetic reasons and in dependence of the amino acids sequence. In the present case, the tryptophan may prevent the peptide to fully tilt into the bilayer.[54]

The biological implications of these observations can be summarized as follows: Vpu and especially the TM part appear to be a highly flexible protein, which senses its lipid environment and easily adapts to it. The lacking lipid dependency of protein structure in the presented simulations can be attributed to this effect. Thus, as suggested earlier,[31] a gating of the channel may rely on the surrounding lipid. Whilst traveling through the Golgi Vpu encounters multiple changes is in the lipid environment. The conformational adaptation may ease the assembly to a multimer, which will become active as a channel at specific sites in the cell.

Vpu's flexibility in the TM part may also allow for interaction with the TM part of other membrane spanning proteins in the HIV infected cell, such as the TASK channel.[55] However, it is up to further investigations whether the association of TM proteins is also via their TM parts or driven solely by the extramembrane parts of the protein.

The position of the kink may be crucial for channeling ions. The assembly of kinked helices may form a vestibule at the C terminus and thereby lower the energy barrier for ions entering the hydrophobic slab of the protein channel. The mechanism of function of such a vestibule has already been evaluated for other channels such as the bacterial K^+ channel KcsB[56] or the nicotinic acetylcholine receptor nAChR.[57] Despite the finding of a kinked helix for the monomer, the assembled "open" channel still may exist with straighter helices.[31]

Conclusion

$Vpu_{1\text{-}32}$ from HIV-1 is a versatile protein, which easily adapts to its environment. The simulations did not show any hydrophobic mismatch for monomeric Vpu peptide with the lipids and possibly also the full length proteins. Rather the peptide/protein is adjusting to the lipid environment. As terminal polar residues anchor the peptide in membrane, it requires the possibility of kinking and tilting to adapt to changes in the lipid environment. It may also be concluded that conformational changes of the peptide are energetically much more favorable than changes of the lipid environment.

The TM part, and possibly also the full length protein, is able to cover large conformational space. This suggests a shallow potential energy well with the consequence of Vpu peptide as a monomeric unit being rather affected than the lipids in its immediate environment.

Acknowledgments

We acknowledge valuable discussions with Anthony Watts (Oxford, UK) and also wish to thank the Paderborn Center for Parallel Computing PC^2 (http://wwwcs.uni-paderborn.de/pc2/) for providing computer time.

References

1. Gonzales, M. E.; Carrasco, L. FEBS Lett 2003, 552, 28.
2. Fischer, W. B. In Protein Reviews; Atassi, M. Z., Ed.; Kluwer Academic/Plenum: New York, 2005.
3. Lu, W.; Zheng, B.-J.; Xu, K.; Schwarz, W.; Du, L.; Wong, C. K. L.; Chen, J.; Duan, S.; Deubel, V.; Sun, B. Proc Natl Acad Sci USA 2006, 103, 12540.
4. Hay, A. J. Semin Virol 1992, 3, 21.
5. Shimbo, K.; Brassard, D. L.; Lamb, R. A.; Pinto, L. H. Biophys J 1996, 70, 1335.
6. Chizhmakov, I. V.; Geraghty, F. M.; Ogden, D. C.; Hayhurst, A.; Antoniou, M.; Hay, A. J. J Physiol 1996, 494, 329.
7. Harada, T.; Tautz, N.; Thiel, H. J. J Virol 2000, 74, 9498.
8. Strebel, K.; Klimkait, T.; Martin, M. A. Science 1988, 241, 1221.
9. Cohen, E. A.; Terwilliger, E. F.; Sodroski, J. G.; Haseltine, W. A. Nature 1988, 334, 532.
10. Friborg, J.; Ladha, A.; Göttlinger, H.; Haseltine, W. A.; Cohen, E. A. J Acc Im Def Syn Hum Retr 1995, 8, 10.
11. Schubert, U.; Schneider, T.; Henklein, P.; Hoffmann, K.; Berthold, E.; Hauser, H.; Pauli, G.; Porstmann, T. Eur J Biochem 1992, 204, 875.
12. Klimkait, T.; Strebel, K.; Hoggan, M. D.; Martin, M. A.; Orenstein, J. M. J Virol 1990, 642, 621.
13. Kimura, T.; Nishikawa, M.; Ohyama, A. J Biochem 1994, 115, 1010.
14. Schubert, U.; Bour, S.; Ferrer-Montiel, A. V.; Montal, M.; Maldarelli, F.; Strebel, K. J Virol 1996, 70, 809.
15. Ewart, G. D.; Sutherland, T.; Gage, P. W.; Cox, G. B. J Virol 1996, 70, 7108.
16. Schubert, U.; Ferrer-Montiel, A. V.; Oblatt-Montal, M.; Henklein, P.; Strebel, K.; Montal, M. FEBS Lett 1996, 398, 12.
17. Maldarelli, F.; Chen, M. Y.; Willey, R. L.; Strebel, K. J Virol 1993, 67, 5056.
18. Federau, T.; Schubert, U.; Flossdorf, J.; Henklein, P.; Schomburg, D.; Wray, V. Int J Peptide Protein Res 1996, 47, 297.
19. Willbold, D.; Hoffmann, S.; Rösch, P. Eur J Biochem 1997, 245, 581.
20. Marassi, F. M.; Ma, C.; Gratkowski, H.; Straus, S. K.; Strebel, K.; Oblatt-Montal, M.; Montal, M.; Opella, S. J. Proc Natl Acad Sci USA 1999, 96, 14336.
21. Wray, V.; Kinder, R.; Federau, T.; Henklein, P.; Bechinger, B.; Schubert, U. Biochemistry 1999, 38, 5272.
22. Henklein, P.; Kinder, R.; Schubert, U.; Bechinger, B. FEBS Lett 2000, 482, 220.
23. Wray, V.; Federau, T.; Henklein, P.; Klabunde, S.; Kunert, O.; Schomburg, D.; Schubert, U. Int J Peptide Protein Res 1995, 45, 35.
24. Kukol, A.; Arkin, I. T. Biophys J 1999, 77, 1594.
25. Grice, A. L.; Kerr, I. D.; Sansom, M. S. P. FEBS Lett 1997, 405, 299.
26. Forrest, L. R.; Kukol, A.; Arkin, I. T.; Tieleman, D. P.; Sansom, M. S. Biophys J 2000, 78, 55.
27. Zhong, Q.; Husslein, T.; Moore, P. B.; Newns, D. M.; Pattnaik, P.; Klein, M. L. FEBS Lett 1998, 434, 265.
28. Sramala, I.; Lemaitre, V.; Faraldo-Gomez, J. D.; Vincent, S.; Watts, A.; Fischer, W. B. Biophys J 2003, 84, 3276.
29. Lemaitre, V.; Ali, R.; Kim, C. G.; Watts, A.; Fischer, W. B. FEBS Lett 2004, 563, 75.
30. Candler, A.; Featherstone, M.; Ali, R.; Maloney, L.; Watts, A.; Fischer, W. B. Biochim Biophys Acta 2005, 1716, 1.

31. Mehnert, T.; Lam, Y. H.; Judge, P. J.; Routh, A.; Fischer, D.; Watts, A.; Fischer, W. B. J Biomol Struct Dyn 2007, 24, 589.
32. Fischer, W. B.; Forrest, L. R.; Smith, G. R.; Sansom, M. S. P. Biopolymers 2000, 53, 529.
33. Park, S. H.; Mrse, A. A.; Nevzorov, A. A.; Mesleh, M. F.; Oblatt-Montal, M.; Montal, M.; Opella, S. J. J Mol Biol 2003, 333, 409.
34. Park, S. H.; Opella, S. J. J Mol Biol 2005, 350, 310.
35. Chandrasekhar, I.; Kastenholz, M.; Lins, R. D.; Oostenbrink, C.; Schuler, L. D.; van Gunsteren, W. F. Eur Biophys J 2003, 32, 67.
36. Nagle, J. F.; Tristram-Nagle, S. Biochim Biophys Acta 2000, 1469, 159.
37. Petrache, H. I.; Dood, S. W.; Brown, M. F. Biophys J 2000, 79, 3172.
38. Lewis, B. A.; Engelman, D. M. J Mol Biol 1983, 166, 211.
39. Forrest, L. R.; Tieleman, D. P.; Sansom, M. S. P. Biophys J 1999, 76, 1886.
40. Sharpe, S.; Yau, W. M.; Tycko, R. Biochemistry 2006, 45, 918.
41. de Angelis, A. A.; Nevzorov, A. A.; Park, S. H.; Howell, S. C.; Mrse, A. A.; Opella, S. J. J Am Chem Soc 2004, 126, 15340.
42. Kovacs, F. A.; Cross, T. A. Biophys J 1997, 73, 2511.
43. Kukol, A.; Adams, P. D.; Rice, L. M.; Brunger, A. T.; Arkin, I. T. J Mol Biol 1999, 286, 951.
44. Wang, J.; Kim, S.; Kovacs, F.; Cross, T. A. Prot Sci 2001, 10, 2241.
45. Marassi, F. M.; Ma, C.; Gesell, J. J.; Opella, S. J. J Magn Res 2000, 144, 156.
46. Khattari, Z.; Arbely, E.; Arkin, I. T.; Salditt, T. Eur Biophys J 2006, 36, 45.
47. Mouritsen, O. G.; Bloom, M. Annu Rev Biophys Biomol Struct 2003, 22, 145.
48. Killian, J. A.; von Heijne, G. TIBS 2000, 25, 429.
49. Ridder, A. N. J. A.; van de Hoef, W.; Stam, J.; Kuhn, A.; de Kruijff, B.; Killian, J. A. Biochemistry 2002, 41, 4946.
50. Ma, C.; Marassi, F. M.; Jones, D. H.; Straus, S. K.; Bour, S.; Strebel, K.; Schubert, U.; Oblatt-Montal, M.; Montal, M.; Opella, S. J. Prot Sci 2002, 11, 546.
51. Tieleman, D. P.; Berendsen, H. J. C.; Sansom, M. S. P. Biophys J 1999, 76, 1757.
52. Yeagle, P. L.; Bennett, M.; Lemaitre, V.; Watts, A. Biochim Biophys Acta 2007, 1768, 530.
53. Kandasamy, S. K.; Larson, R. G. Biophys J 2006, 90, 2326.
54. Özdirekcan, S.; Rijkers, D. T. S.; Liskamp, R. M. J.; Killian, J. A. Biochemistry 2005, 44, 1004.
55. Hsu, K.; Seharaseyon, J.; Dong, P.; Bour, S.; Marbán, E. Molec Cell 2004, 14, 259.
56. Doyle, D. A.; Cabral, J. M.; Pfuetzner, R. A.; Kuo, A.; Gulbis, J. M.; Cohen, S. L.; Chait, B. T.; MacKinnon, R. Science 1998, 280, 69.
57. Miyazawa, A.; Fujiyoshi, Y.; Unwin, N. Nature 2003, 423, 949.